NUMERICAL SIMULATION STUDY OF HYDRODYNAMIC IMPACT OF SEA-CROSSING BRIDGE

Xiao-Feng Guo
Third Institute of Oceanography, State Oceanic Administration, Xiamen, Fujian, P.R.C.

Chu-Han Chen
Third Institute of Oceanography, State Oceanic Administration, Xiamen, Fujian, P.R.C., chenchuhan@tio.org.cn

Jun-Jian Tang
Third Institute of Oceanography, State Oceanic Administration, Xiamen, Fujian, P.R.C.

Zhou-Hua Guo
Third Institute of Oceanography, State Oceanic Administration, Xiamen, Fujian, P.R.C

Recommended Citation

NUMERICAL SIMULATION STUDY OF HYDRODYNAMIC IMPACT OF SEA-CROSSING BRIDGE

Xiao-Feng Guo, Chu-Han Chen, Jun-Jian Tang, and Zhou-Hua Guo

ABSTRACT

This paper used the Sea-Crossing Bridge in Quanzhou Bay as an example to simulate its tidal flow field after construction by a semi-implicit Lagrangian-Eulerian finite difference method. Triangle or quadrilateral meshes were used to refine a mesh for the sea area close to the bridge in the model. Each bridge pier was treated as land. The minimum side length of the mesh was approximately 5 meters. The simulation results showed that slow flow areas were formed in front of bridge piers due to the influence of rising and falling tides; at the back of bridge piers, slow flow areas were also formed after rising and falling tides passed the piers. The tide race direction of rise and fall in the main bridge area was basically perpendicular to the bridge site line. The influence domain of upstream and downstream flow along the bridge site line could extend approximately 1 km away. The variation of annual siltation intensity was mainly located in the water area around the bridge piers. The annual siltation intensity of suspended sediment around the main bridge pier increased about 2-20 cm/year. The annual siltation intensities between piers decreased about 1-2 cm/year. The movement of tidal flow and the variation of sediment back-siltation rule would have certain impacts on the marine ecosystem, regional flood control, and navigation in Quanzhou Bay.

I. INTRODUCTION

In recent years, with the rapid development of marine economy, many sea-crossing bridges have been built in the coastal areas of China. After completion of sea-crossing bridge construction, the bridge piers submerged in the ocean resulted in the increase of flow resistance adjacent to the bridge and the decrease of the water-carrying section, which had certain impacts on the tidal flow field of the marine environment adjacent to the bridge site, and also influenced seabed erosion and siltation (Pang et al., 2008a; 2008b) and thus affected the marine environment.

The hydrodynamic impact of a sea-crossing bridge can be studied through a numerical simulation method. Due to the relatively small dimensions of bridge piers, approximately 3 to 30 meters, the generalization of the pier (Pang et al., 2008a) should be taken into special consideration when studying the numerical computation regarding hydrodynamic impact of bridge piers on marine or tidal river environments. Existing treatment methods (Tang and Li, 2001; Chen and Hu, 2003; Cao et al., 2006; Yuan and Xu, 2006; Zhang et al., 2007) mostly include mesh refinement within a certain extent adjacent to bridge piers, then carry out numerical simulation by the additive roughness method, the water-blocking area replacement method, and the additive resistance method, etc. These methods mostly simulate the hydrodynamic effect through increasing friction-resistance coefficient and decreasing water depth based on water-resistance extent; however, they could not characterize the local flow field adjacent to the bridge piers. Therefore, the computation based on these simulation methods differs from engineering actuality, which causes the computational results to have a higher rate of error.

This research used a semi-implicit Lagrangian-Eulerian finite difference method and triangle or quadrilateral meshes to accurately simulate the hydrodynamic environmental impact of sea-crossing bridge construction on a marine area. Each bridge pier was treated as land, with minimum mesh side length of about 5 m, to obtain the refined tidal flow field adjacent to the bridge piers. Based on the predication of hydrodynamic impact, this paper analyzed and assessed the marine environmental impact of sea-crossing bridge construction (Li et al., 2008).

II. PROJECT BACKGROUND

Quanzhou Bay is located off the middle of the south-eastern coast of Fujian Province; it is surrounded by Huian County on the north-eastern side, Quanzhou City on the north-western
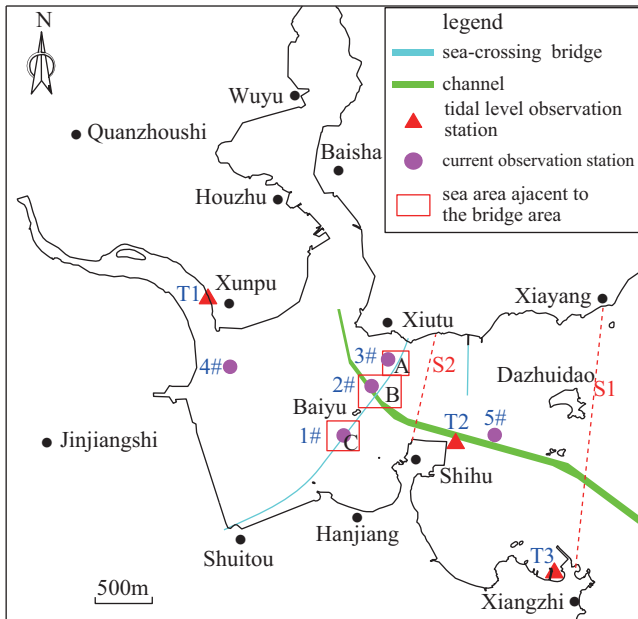
Fig. 1. **Quanzhou Bay sea crossing bridge and hydrological observation station locations.**

side, Jinjiang City and Shishi City on the south-western, and is adjacent to the Taiwan Strait on the eastern side. There is mouth bar development at the bay front, which opens to the south-east and has large and small individual islands. Quanzhou Bay belongs to an open bay (Fig. 1) and has a long and tortuous coast line with an overall length of 80.18 km and a bay area of 128.18 km^2, of which sea beach area is up to 80.42 km^2, and water area is up to 47.46 km^2. Quanzhou Bay is a semi-closed bay located where the Jin River and Luoyang River enter the sea. Its sediment was mainly brought by the discharge of the Jin River runoff and sands from outside the bay by tidal rise and fall. The former is the major source of Quanzhou Bay sediment.

The total length of the Quanzhou Bay Sea-Crossing Bridge is about 12.71 km. The bridge crosses the sea from adjacent to the Jin River head, passes through the eastern side of Baiyu Island and the center of the main channel of Quanzhou Bay, and ends at the Xiutu coast. The length of bridge over the ocean is 9.7 km as shown in Fig. 1. The main navigation bridge has a main span of 400 m and was built as a pre-stressed concrete, cable-stayed bridge, with double towers and double cable planes. The pilot bridge in the deep water area was built from 70 meters of pre-stressed concrete, a continuous box girder with 7 sections, and 240 bridge piers (State Oceanic Administration Third Institute of Oceanography, 2010).

III. PROFILE OF NATURAL ENVIRONMENT

With its wide mouth, winding shorelines, and alternating headlands, Quanzhou Bay is characterized by its regular semi-diurnal tides, which have a mean range of 4.27 m. The tidal currents in Quanzhou Bay are reciprocating tidal currents,

which are relatively stable. The tidal currents flow into the bay at high tide and flow out of the bay at low tide. Waves in Quanzhou Bay are mainly mixed waves formed by wind waves in the NNE-NE and SSW directions and surges of SE direction. They have a monthly average wave height of 0.7-1.1 m and an average wave period of 3.7-4.2 s, measured across years. Quanzhou Bay is a semi-closed bay joined by Jinjiang River and Luoyang River. Its sediment comes mainly from the sediment brought by the runoff from Jinjiang River, which is the main source of sediments in Quanzhou Bay and the sediment that flows into the bay with tide currents at high tide. The average sediment concentration of 5 hydrometric stations in February 2009 was 0.1029 kg/m^3 during spring tide, 0.0513 kg/m^3 during middle tide, and 0.0377 kg/m^3 during neap tide. The average sediment concentration during middle tide was lower than that during spring tide but higher than that during neap tide. The suspended sediments in different parts of Quanzhou Bay, categorized into fine-grained sediments, have roughly the same average median particle diameters of about 0.0l mm.

Sediment samples taken from Quanzhou Bay include coarse sand, medium-coarse sand, medium sand, medium-fine sand, clayey sand, and sandy clay, among which, medium-coarse sand, medium-fine sand, and sandy clay found in the bottom sediments in the middle part of the bridge indicate that such hydrodynamic conditions as tide currents and wind waves are relatively strong there. Sandy sediments found on the northern side of the beach indicate that the impact of wind waves and tide currents are also strong there. Clayey sand found on the southern side of the tidal flat indicates that the hydrodynamic conditions there are relatively weak.

III. NUMERICAL SIMULATION OF HYDRODYNAMIC IMPACT PREDICTION

1. Tidal Current and Sediment Control Equation and its Numerical Solution

Two-dimensional shallow water equations in plane rectangular coordinate were utilized to simulate the tidal current field. With reference to the sediment transport equations under the combined influence of wave and tide derived by Dou (1999) and considering the dynamic diffusion effect, the two-dimensional mean suspended sediment transport equations and seabed deformation equations were derived, and the corresponding tidal current and sediment equations are as follows:

$$\frac{\partial \eta}{\partial t} + \frac{\partial}{\partial x}(Hu) + \frac{\partial}{\partial y}(Hv) = 0 \qquad (1)$$

$$\frac{\partial u}{\partial t} + u\frac{\partial u}{\partial x} + v\frac{\partial u}{\partial y} = -g\frac{\partial \eta}{\partial x} + fv - ru + A_x\left(\frac{\partial^2 u}{\partial x^2} + \frac{\partial^2 u}{\partial y^2}\right) \quad (2)$$

$$\frac{\partial v}{\partial t} + u\frac{\partial v}{\partial x} + v\frac{\partial v}{\partial y} = -g\frac{\partial \eta}{\partial y} - fu - rv + A_y\left(\frac{\partial^2 v}{\partial x^2} + \frac{\partial^2 v}{\partial y^2}\right) \quad (3)$$

$$\frac{\partial HS}{\partial t} + \frac{\partial HuS}{\partial x} + \frac{\partial HvS}{\partial y} + \alpha \omega_s (S - S_*)$$

$$= \frac{\partial}{\partial x}(HD_x \frac{\partial S}{\partial x}) + \frac{\partial}{\partial y}(HD_y \frac{\partial S}{\partial y}) \tag{4}$$

$$\gamma' \frac{\partial \eta_s}{\partial t} = \alpha \omega_s (S - S_*) \tag{5}$$

Where, x and y are plane rectangular coordinates; t is time; H is water depth ($H = d + \eta$); d is the water depth beneath the mean water level; η is the water level; u and v are the directional components in x and y directions, respectively; $u = (1/H)\int_{-h}^{\eta} u' dz$ and $v = (1/H)\int_{-h}^{\eta} v' dz$ are the average flow velocities along water depth, respectively; g is the gravitational acceleration; f is the Coriolis parameter; r is the bottom friction coefficient; c_n is the Chézy coefficient, which is equal to $c_n = H^{1/6}/n$ in $r = g\sqrt{u^2 + v^2}/c_n^2 H$; n is the roughness coefficient of the seabed, $n = 0.02$; Ax and Ay are the viscosity coefficients of horizontal movements and are calculated using the Smagorinsky formula:

$$A_x = C\Delta x \Delta y [(\partial u/\partial x)^2 + (\partial u/\partial x + \partial u/\partial y)^2 / 2 \\ + (\partial u/\partial y)^2]^{1/2} , \text{C} \approx 0.1\text{~}0.2,$$

and Ay can also be calculated in the same way.

S is the vertical mean sediment concentration; S_* is the sand-carrying capacity under the combined influence of wave and tide; ω_s is the settlement velocity of suspended sand particles; D_x and D_y are the sediment dispersive coefficients in the x and y directions, respectively; $\gamma' = 1750 d_{50}^{0.183}$ is the dry density of suspended sediment; α is the settlement probability of suspended sediment particles; and η_s is the erosion and siltation thickness caused by suspended sediment.

Eqs. (1) - (5) were solved by the semi-implicit finite difference method (Casulli and Cheng, 1992; Casulli and Cattani, 1994; Oliveira and Baptista, 1995; Casulli and Zanolli, 1998; Zhang et al., 2004; Tang et al., 2006; Tang et al., 2011) proposed by Vincenzo Cassulli. This method utilizes non-structural triangle or quadrilateral orthogonal meshes for modeling. Each side of triangle (or quadrilateral) mesh was the boundary of another triangle (or quadrilateral) mesh. The central lines of adjacent meshes were perpendicular to the boundary sides. In the course of solving the model, implicit finite difference components in equations were favorably selected, and the Lagrangian-Eulerian method was used to decompose transport components and horizontal viscosity components; thus, the time step of the solution would not be limited by the CFL condition and could be amplified in comparison with other methods. This method can assure the stability of the solution (Tang et al., 2011). When the model is applied to bridge construction, smaller sides can be used for the bridge pier meshes, and the

time step can be longer (20 s); this treatment can assure the stability of the solution and also improve the computational efficiency. Minimum mesh sides of 5 m were used in this paper. Coastal waters have wide tidal areas, which are submerged when the tide rises and emerge when the tide falls. In the modeling computation, beach exposure was treated as a dynamic boundary condition. A non-flow passing technique was used in the model to automatically judge and treated the dry-wet element, dry-wet side, and dry-wet nodal.

2. Boundary Conditions and Parameter Selection

The coastline is a solid boundary. The flow velocity in the normal direction is zero. There are two cross-sections in the fluid open boundary of open sea: one control point is secured as the SE point at the southeast corner of the computational marine space; the connecting line of Weitou and the SE point are south of the open boundary section; and to the east is the connecting line of the SE point and Chongwu. The water depth of the open boundary is provided by the tide level of the tidal current field at the Taiwan Strait.

Boundary conditions of suspended sediment field: shore boundary: $\frac{\partial S}{\partial n} = 0$, where n is the normal direction of the shore boundary.

Water boundary:

Flow into computational domain: $S(x, y, t) = S_{in}(x, y, t)$, where S_{in} is the given measured value of sediments in the water boundary.

Flow out of computational domain:

$$\frac{\partial(HS)}{\partial t} + \frac{\partial(HUS)}{\partial x} \frac{\partial(HVS)}{\partial y} = 0$$

Values in the open boundary of the sediment field: 0.44 kg/m³ serves as the sediment concentration in the river mouth of Jinjiang River; 0.03 kg/m³ (spring tide), 0.02 kg/m³ (middle tide), and 0.012 kg/m³ (neap tide) were taken as the sediment concentration in the eastern open boundary of open sea of construction site (Gaoleishan section); 0.03 kg/m³ (spring tide), 0.02 kg/m³ (middle tide), and 0.012 kg/m³ (middle tide) were taken as the sediment concentration in the southern open boundary of open sea of construction site (Cuoshang section).

Sediment transport capacity of flow S_*: In the sediment transport equation, the quantity of sediment that surges from the surface of seabed is indicated by sediment transport capacity S_*. Dou Guoren has put forward a formula for sediment transport capacity under the combined action of tide currents and wave currents:

$$S_* = \alpha \frac{\gamma \gamma_s}{\gamma_s - \gamma}(\frac{V^3}{C^2 h\omega} + \beta \frac{H^2}{hT\omega})$$

In this formula, γ and γ_s are the volume weights of water
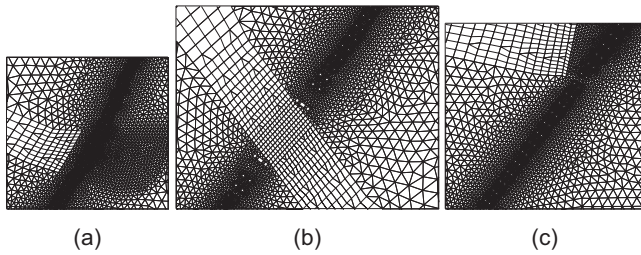
Fig. 2. Schematic of local mesh around the bridge piers ((a): Partial north deep-water area; (b): Partial main bridge area; (c): Partial south deep-water area).

Fig. 3. Quanzhou Bay Sea area of the non-structural mesh expansion schematic.

and sediment particles respectively; ω is the settling velocity; C is the Chezy coefficient; h is the water depth; V is the flow velocity; H is the wave height; and T is the wave period. α and β coefficients are calibrated according to the investigation data of flow and sediment.

The settling velocity ω is 0.05 cm/s. Coefficient of saturation recovery α: coefficient of saturation recovery is the parameter indicating the recovery velocity of sediment concentration in the body of water to sediment transport capacity when the transportation of suspended loads of sediment takes place in a body of water. The following formula was used to perform the calculation:

$$\alpha = 2\varphi(\frac{\gamma'\omega_s}{\sigma}) - 1$$

In the formula, $\varphi(\frac{\gamma'\omega_s}{\sigma})$ is the probability function; $\sigma \approx 0.033\, u_*$ is the mean squared error of vertical fluctuating velocity; u_* is the friction resistance velocity; $\gamma' = \sqrt{\frac{\rho_s - \rho_w}{\rho_w}}$, ρ_s is the volume-weight of fine-grained sediment coagulation, ρ_w is the volume-weight of water.

2. Generalization of the Treatment of Bridge Piers

Existing generalization treatment methods (Tang and Li, 2001; Chen and Hu, 2003; Cao et al., 2006; Yuan and Xu, 2006; Zhang et al., 2007), such as the additive roughness method, water-blocking area replacement method, and additive resistance method could not precisely characterize the local flow field adjacent to the bridge piers. In this study, to accurately reflect the tidal current field adjacent to the bridge piers, the meshes were refined on both sides of the bridge site during the process of simulation. The refined minimum meshes were up to 5 m. The foundation of every bridge pier was treated as a polygon or rectangular island-like solid for meshing, i.e., the bridge foundation was treated as land in the simulation. The shape of the island solid was mostly based on the shape of the pile cap. Conservatively, the boundary sizes of the island-like solid were slightly greater than those of the pile cap. The local mesh near the bridge piers are shown in Fig. 2.
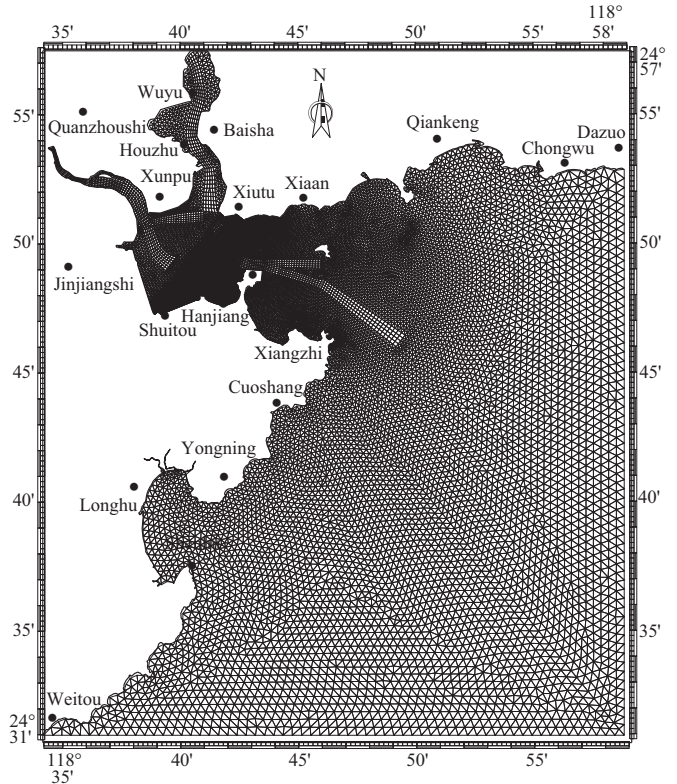
In Fig. 2, A, B, and C are the typical local mesh schematics near the bridge piers of the approach bridge in the north deep water area, the main bridge, and the approach bridge in the south deep water area, respectively. The main bridge piers were represented by rectangular and square solids with dimensions of 20 × 24 m, 18 × 18 m, and 14 × 14 m, respectively. Every pier of the approach bridge in the north and south deep water areas was represented by a two square solid with dimensions of 10.2 × 10.2 m.

4. Computational Domain and the Associated Identification of the Model

Fig. 3 shows the simulated computational scope of the extended marine space and non-structural mesh schematics for Quanzhou Bay, which includes the marine space to the east of Weitou, south of Chongwu, and the entire Quanzhou Bay. Meshes were refined for the marine space near the Quanzhou Bay Bridge construction site. The maximum mesh side was about 1,000 m, and the minimum side was about 5 m. The overall mesh nodal was about 30,000 with approximately 50,000 meshes.

The observed data for tidal level and tidal current were taken from flow measure of the 2009 spring tide and real-testing data of the synchronization tidal level. The location of the hydraulic observation station is shown in Fig. 1. Tidal level stations were located at Xunfu, Shihu, and Xiangzhi. There were five tidal current and sediment stations. Stations 1 through
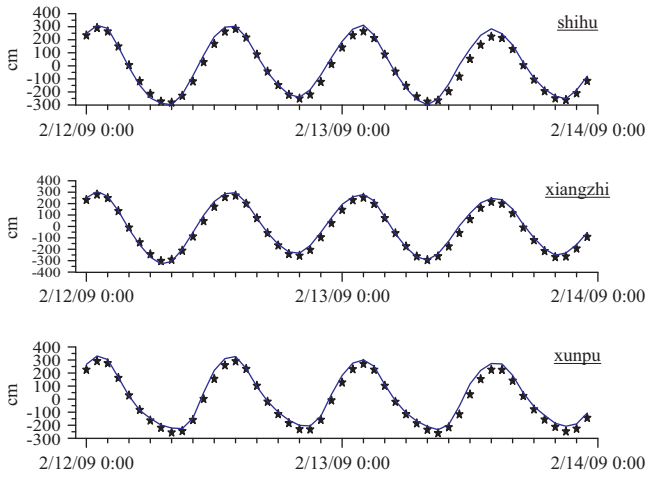
Fig. 4. Curves of simulated and observed values from tidal level stations.
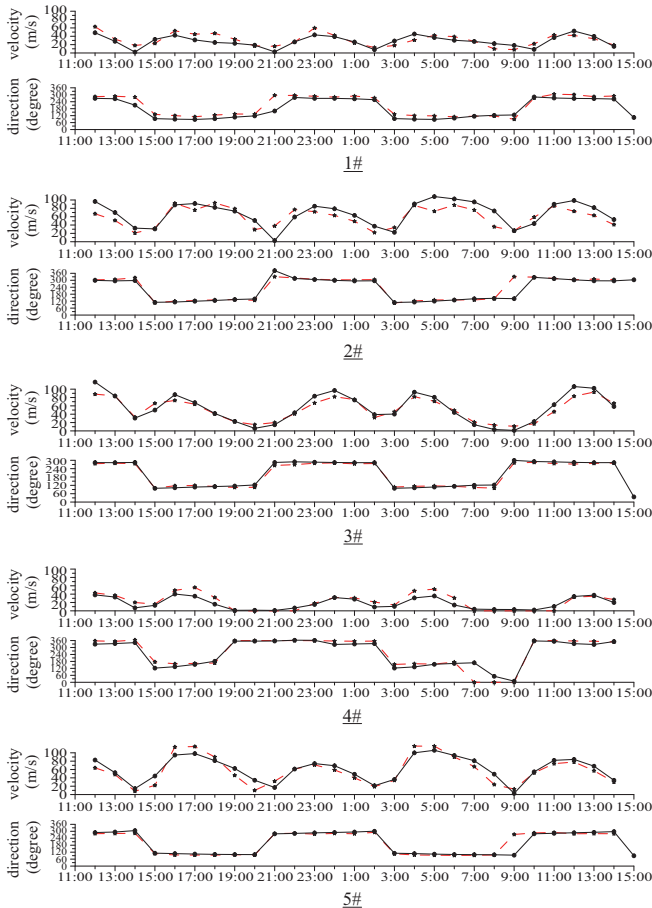
Fig. 5. Simulation and experimental validation curves from tidal current stations.

Fig. 6. Process curve and the simulated values of the average sediment concentration in the vertical for an actual sediment station.

3 were located at the west side of the bridge site, station 4 was located at the Jin River estuary on the southeastern side of Xunfu, and station 5 was located at the edge of the main navigation channel of the bridge site and the south side of Xiesha.

Fig. 4 shows the computational and observed data for the tidal level during flow measurements of the spring tide at the Xunfu, Shihu, and Xiangzhi temporary tidal level stations in February 2009. It shows a basic match between computational values and observed values in the tidal curve. Fig. 5 shows the identification curve diagram between the simulation values and the observed values at tidal current stations No.1 through 5 in February 2009. In general, the computational values basically matched with observed values in flow velocity and direction. Fig. 6 shows the variation process curve of sediment concentration versus time from hydrology and sediment stations No.1 through 5 for the spring tide in February 2009. The observed sediment concentration values at various stations were basically close to the computational vertical average sediment concentration; therefore, the identification results from numerical simulation indicated the simulation model satisfactorily reflected the tidal sediment movement in Quanzhou Bay and could be used for the computation of construction.

5. Numerical Simulation of Tidal Sediment

1) Summary of Numerical Simulation Plan

The Quanzhou Bay Sea-Crossing Bridge was located at the marine space in the west of Shihu, Quanzhou Bay. The west marine space of Qianjiang is a large shoal area with water depth of 0 to 4 meters. The south side of Baiyu has a water depth of 0 to 2 meters. The main channel at the north of Baiyu has a water depth of 4 to 8 meters. The shoal area off the Xiutu coast has a water depth of 0 to 4 meters. To illustrate the impact of construction on the tidal prism of Quanzhou Bay, the S1 section obtained from Xiangzhi-Xiayang of the Quanzhou estuary and the S2 section obtained from Shihu-Xiutu were marked to compute the flow of the next periodic tide. The S1 and S2 sections are shown in Fig. 1. This simulation included two plans as described below:

Table 1. Sectional flow comparison during one period of spring tide rise and fall after construction.

Plan		Tidal Fall (×10⁸ m³)		Tidal rise (×10⁸ m³)	
		S1	S2	S1	S2
Existing status	Spring tide	6.260	3.398	6.164	3.320
Bridge Proejct	Spring tide	6.254	3.392	6.158	3.314
	Increase and decrease	-0.006	-0.006	-0.006	-0.006
	Percentage	-0.1	-0.2	-0.1	-0.2

(a) Pre-construction: On the existing costal line, the planed Shihu construction areas 1 through 10 have started construction. The construction areas were formed by backfilled beach, andthe Xiesha artificial island has started to be backfilled.

(b) Post construction: On the basis of the pre-construction plan, the Quanzhou Bay Sea-Crossing Bridge construction was started.

2) Pre-Construction Simulation Result

The flow velocity distribution included various stages of a strong deep channel, weak shoal, and rapid rise. The flow velocity of the Xiesha north channel was about 0.4 to 0.8 m/s; the deep channel flow velocity at the Shihu frontier was about 1.0 to 1.2 m/s; the velocity at the marine space near the north channel of Baiyu Island was around 0.8 m/s, and the flow velocity at the rapid fall stage was less than that at the rapid rise stage; the flow velocity in the marine space to the south of Baiyu was about 0.6 to 1.0 m/s, and the flow velocity at the rapid fall stage was less than that at the rapid rise stage.

After construction of a planned artificial island and the Shihu construction area, the flow velocity was strengthened at the construction area at the north channel of the artificial island and Shihu and channels between the artificial islands. Tidal fall accelerated the sediment transport out of Quanzhou Bay. Compared to the existing coast line, the sediment concentration and annual siltation intensity were slightly decreased at the Shihu construction area and the channels between the artificial islands. There was no significant variation for the sediment concentration and annual siltation intensity in the marine space in the western part of the Xiutu-Shihu Section. The annual siltation intensity of the main navigation channel to the north of Baiyu Island was about 20-30 cm/year, and the annual siltation intensity of the main navigation channel to the south of Baiyu Island was about 5-20 cm/year.

3) Post Construction Simulation Results

After the start of the Quanzhou Bridge construction, the existence of marine bridge piers would cause flow variations of tide rise and fall. Table 1 shows the comparison of sectional with bridge construction. From Table 1, the flow passing the S1 section for spring tide rise and fall prior to construction were 6.26 × 10⁸ m³ and 6.164 × 10⁸ m³, respectively; and the flow passing the S2 section for spring tide rise and fall prior to
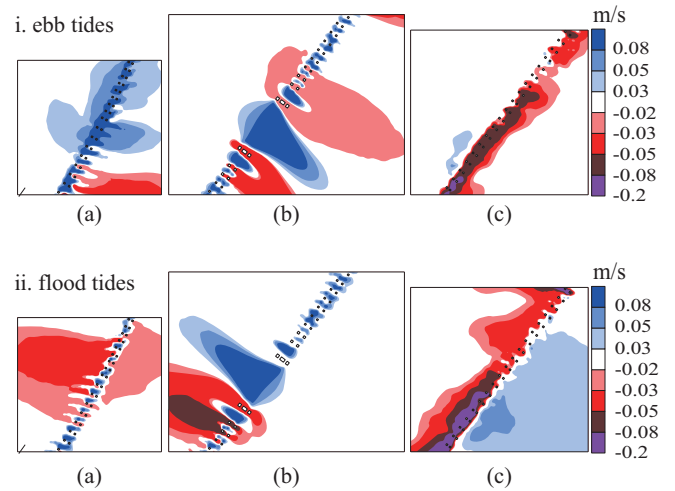
Fig. 7.   Isoline distribution of flow velocity variation near the bridge site before and after bridge construction.
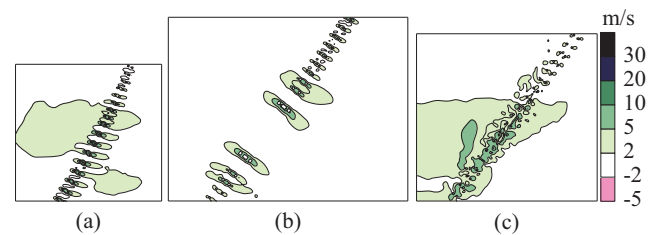
Fig. 8.   Annual suspended sediment variation distribution near the bridge site before and after bridge construction.

construction were 3.398 × 10⁸ m³ and 3.320 × 10⁸ m³, respectively. After construction of bridge project, the average flow of spring tide rise and fall for the S1 and S2 sections decreased by about 6 × 10⁵ m³ or approximately 0.1% to 0.2%. This observation indicated that the construction of the Quanzhou Bay Bridge project has no significant impact on the tidal prism of Quanzhou Bay, and it also has no impact on the water exchange between the outside and inside of the Bay.

After the construction of the Quanzhou Bridge project, the maximum variation in the tidal level in the areas upstream and downstream of the bridge was within 2 cm, which indicates that the project had little influence on tidal level.

Fig. 7 shows the isogram distribution of flow velocity variation during tide rise and fall prior to and after bridge construction. From Fig. 7, it was observed that compared to the existing condition the flow velocity variation area is mainly concentrated between the bridge piers and the waters near the piers after the bridge construction starts. The greatest distance upstream and downstream away from the bridge lines for which the waters are influenced by the bridge was about 1 km.

(a) Tide fall period of time: The tide fall direction for the main bridge area and the waters adjacent to the north deep water area was towards the SE. The tide fall velocity, in the SE direction, around the slow flow area of bridge piers de-

creased, and the flow direction changed. Within the 400 m slow flow area in the SE direction, the flow velocity decreased by about 0.02-0.3 m/s. The flow velocity of the channels between the main bridge piers increased by about 0.03-0.15 m/s, and the flow direction changed by about 2-4° clockwise. The flow velocity between the auxiliary piers of the main bridge increased by about 0.03-0.2 m/s. Since the water level for the waters between the south of Baiyu and Ganjiang is relatively shallow with a complicated tidal flow direction and is not perpendicular to the bridge line by a certain angle, the flow velocity for the waters between two sides of the bridge line and the piers decreased. The tide fall in the slow area around the bridge piers was in an E to NE direction, and the flow velocity for the tide along the bridge piers was in an E to NE direction and decreased by about 0.02-0.2 m/s.

(b) Tide rise period of time: The tide rise flow was in an inverse direction of the tide fall. The tide flow for the waters to the north of Baiyu Island was mainly in a NW direction. The changes for flow velocity and direction during tide rise were similar to those during tide fall, but the direction was opposite. The flow velocity of the NW side in the tide rise direction for the main bridge area to the north of Baiyu Island and the piers around the waters of the approach bridge in the north deep water area generally decreased by about 0.02-0.3 m/s. The flow velocity between the piers increased by about 0.03-0.15 m/s. The flow of the main channel between the piers during tide rise changed 1-3° clockwise. The tide rise flow in the south waters of Baiyu Island was mainly in a W to SW direction, and the flow velocity along the bridge line for the south deep water area during tide rise decreased by 0.02-0.2 m/s.

In order to compare the variation of annual suspended sediment intensity prior to and after construction, the annual sediment intensity variation isogram curve was made by subtracting the annual suspended sediment intensity at each nodal point prior to construction from those after construction as shown in Fig. 8. From Fig. 8, it was observed that the annual suspended sediment intensity around the main bridge piers increased by about 2-20 cm/year. The pier diameters, except for that of the main bridge pier, were relatively small, which resulted in an increase in the annual suspended sediment intensity around these piers of about 2-5 cm/year, and a decrease in the annual suspended sediment intensity between these piers of about 1-2 cm/year. The annual suspended sediment intensity for the waters on the north side of the artificial island increased by about 2-5 cm/year. The variation of the annual suspended sediment intensity for the waters near the bridge site was mainly correlated with the variation of flow velocity prior to and after construction. Tide rise and fall currents resulted in the formation of slow flow areas around the bridge piers in the tidal flow direction. The flow velocity in front of and behind the piers decreased, but the flow velocity between the piers increased. Subject to the impact of flow flush, the annual suspended

sediment intensity in front of and behind the bridge piers increased, but it decreased between the bridge piers.

V. IMPACT OF HYDRODYNAMIC CONDITION CHANGE ON MARINE ENVIRONMENT

The construction of the Quanzhou Bay Sea-Crossing Bridge would directly alter the regional tide movement characteristics and lead to changes in sediment erosion and deposition as well as the migration rule of pollutants. It would affect the marine ecosystem, flood prevention, and navigation (Liu et al., 2003).

1. The Impact Analysis on the Marine Ecosystem

Quanzhou Bay has wide sea area with a large beach, abundant biodiversity, and a sensitive ecological environment. It is a beach wetland typical of sub-tropic estuaries in China and is within the province of the natural protection area of the Quanzhou Bay Wetland Estuary. After construction of the Quanzhou Bay Sea-Crossing Bridge, the flow velocity and flow pattern of the original tide flow field would be altered, and the tidal prism would be decreased so as to decrease the water's environmental capacity and the pollutant diffusion capacity of the marine environment, thus intensify the accumulation of pollutants in the marine environment (Sun et al., 2002), decrease biodiversity, and affect the integrity of the tidal flat wetland in Quanzhou Bay. Meanwhile, the alteration of the flow field would also lead to local seabed siltation, which would cause beach erosion, alter the types of marine sediments, affect the habitats of benthos organisms, and affect coastal tourism resources (Yang and Xue, 2004). After the completion of the project, the sectional flow of rise and fall of spring tide in a tidal cycle decreased by 0.1-0.2%. In this way, the project had only a limited impact on water exchange capacity of Quanzhou Bay and little influence on the marine ecosystem.

2. Impact on Flood Prevention

The sea-crossing area of the Quanzhou Bay Bridge is the spillway passage of the Quanzhou Bay estuary. After construction, the bridge led to the reduction of the water-carrying section of Quanzhou Bay, which resulted in lower elevation of previously high water, higher elevation of previously low water, a decrease in the tidal dynamics, and a reduction of the tidal prism for the waters upstream of the bridge and the Quanzhou Bay waters. In general, construction of the bridge led to a decrease in flow velocity of upstream waters and in sediment transport capacity. In addition, the construction readily accelerated sediment accumulation in the water passage and Quanzhou Bay raising the seabed, which had an unfavorable impact (Peng, 2002) on flood prevention, flood discharge, tidal accommodation, and drainage, etc. for the upstream area.

3. Impact on Navigation

The navigation channel of Quanzhou Bay crosses the main bridge pier of the Quanzhou Bay Sea-Crossing Bridge. After

construction, the annual suspended sediment intensity around the bridge site gradually decreased due to the impact of water flushing through, but the sediment back-siltation of the navigation channel 100 meters away from both sides of the bridge site slightly increased; therefore, the sediment siltation had a small impact on navigation.

VI. CONCLUSION

This paper utilized a numerical simulation method to predict the effects of the Quanzhou Bay Sea-crossing Bridge on the hydrodynamics of the marine space, which include the tidal level, sectional flow of the rising and falling tides, variation in tidal flow velocity and erosion and siltation of suspended sediment in the water surrounding the construction site before and after the construction project. Based on the simulation, this research further conducted an analysis of the impact on the marine environment.

Regarding the prediction of the hydrodynamic impact, this research utilized a refined mesh method to simulate the impact of the bridge piers, which were treated as land, and obtained the local tidal flow field as well as the sediment erosion and deposition field adjacent to the bridge piers. The results of the simulation indicated the following:

(a) The current of the tidal rise and fall formed slow flow area in front of the bridge pier; after passing the piers, it also formed a slow flow area behind the piers; the flow direction of the rapid rise and fall tides in the main bridge site was basically perpendicular to the bridge line; and the farthest distance upstream and downstream of the bridge line for which the flow velocity of the waters was influenced was up to 1000 meters away from the bridge line.

(b) The area of variation of annual suspended sediment intensity was mainly located at the waters in front of and behind the bridge piers; the annual suspended sediment intensity in front of and behind the bridge piers increased by about 2 to 20 cm/year; the bridge pier diameter except for the main bridge pier was relatively small, and the corresponding annual suspended sediment intensity in front of and behind the bridge piers increased by about 2 to 5 cm/year; and the annual sediment intensity between the bridge piers decreased by 1 to 2 cm/year.

Construction of the Quanzhou Bay Sea-Crossing Bridge project altered the regional tidal movement characteristics, led to the variation of sediment erosion and deposition and the pollutant migration rule, and produced a certain impact on the marine ecosystem, regional flood prevention, and navigation activities. The prediction of the impact of engineering construction on marine hydrodynamics is the basis of marine environmental assessment. This paper brought bridge construction into the simulation, and conducted valuable exploration into how precisely the simulation reflected the impact of bridge construction on the marine environment. The next step

of this research should track the monitoring data after construction completion and validate the simulation results to further identify the model parameters (Guo et al., 2014).

REFERENCES

Cao, M. X., X. R. Gan, F. N. Zhou and X. H. Wang (2006). Numerical computation and analysis of the impact of bridge piers in tidal river on water flow. Journal of Yangtze River 37, 81-84. (in Chinese)

Casulli, V. and E. Cattani (1994). Stability, accuracy and efficiency of a semi-implicit method for three-dimensional shallow water flow. Computers & Mathematics with Applications 27, 99-112.

Casulli, V. and R. T. Cheng (1991). Semi-implicit finite difference methods for three-dimensional shallow water flow. International Journal for Numerical in Fluids 15, 629-648.

Casulli, V. and P. Zanolli (1998). A three-dimensional semi-implicit algorithm for environmental flows on unstructured grids. Proceedings of the Conference On Numerical Methods for Fluid Dynamics, University of Oxford, Oxford, England, 57-70.

Chen, X. J. and C. H. Hu (2003). Research on plenar 2-D mathematical model of bridge pier choked flow. Journal of China Institute of Water Resources and Hydropower Research (3), 194-199. (in Chinese)

Dou, G. R. (1999). Re-exploration of sediment incipience velocity. Journal of Sediment Research 6, 1-9. (in Chinese)

Guo, X. F., C. Wang, C. H. Chen and J. J. Tang (2014). Numerical simulation of suspended sediment transport during construction of Meizhou Bay peak tail reclamation project. Journal of Applied Oceanography 33, 125-132. (in Chinese)

Li, P. S., G. Z. Xie, X. H. Chen and M. X. Jiang (2008). The application of numerical simulation method in marine environmental impact assessment. Journal of Hainan Normal University (Natural Sciences) 21, 200-207. (in Chinese)

Liu, Y., F. Gong and B. Xia (2003). Focus on ecological risk of land reclamation. Journal of Environmental Science Trends (4), 25-27. (in Chinese)

Oliveira, A. and A. M. Baptista (1995). A comparison of integration and interpolation Eulerian-Lagrangian methods. International Journal of Numerical Methods in Fluids 21, 183-204.

Pang, Q. X., M. G. Li and M. Mai (2008a). Impact study of bridge piers on the adjacent marine hydrodynamic enviroment. Journal of China Harbour Construction 1, 32-35. (in Chinese)

Pang, Q. X., X. J. Zhuang, Z. H. Huang and J. C. Sun (2008b). Study on numerical simulation of hydrodynamic conditions influenced by pier in sea. Journal Waterway and Harbor 29, 16-20. (in Chinese)

Peng, S. Y. (2002). Shenzhen river estuarine reclamation on flood control and river bed scouring and silting influence research. Journal of Ocean Engineering 20, 103-108.

State Oceanic Administration Third Institute of Oceanography, State Oceanic Administration (2010). Environmental Influence Statement of Quanzhou Bay Sea-Crossing Passage Project. Xiamen, Third Institute of Oceanography, State Oceanic Administration. (in Chinese)

Sun, C. Q., X. C. Wang, Y. L. Sun and G. A. Lou (2002). Study on impact of Jiaozhou Bay sea-filling on hydrodynamic environment. Journal of Marine Science 26, 47-50. (in Chinese)

Tang, J., C. Chen and S. Wen (2011). Numerical Simulation of Tidal Flow Field for Quanzhou Bay Sea-Crossing Bridge. China Marine Engineering Society, The Fifteenth Session of the Chinese Marine (Coastal) Engineering Symposium, edited by Chinese Ocean Engineering Society, Beijing, Marine Press. (in Chinese)

Tang, J. J., S. H. Wen and C. H. Chen (2006). two dimensional tidal flow field numerical simulation of haitan strait. Journal of Taiwan Strait 25, 533-540. (in Chinese)

Tang, S. F. and P. Li (2001). Numerical simulation study of tidal flow under impact of pile groups resistance. Journal of China Harbour Construction 1, 25-29. (in Chinese)

Yang, X. A. and X. Z. Xue (2004). Cumulative impact assessment on coastal

engineering: a case study of xiamen western sea. Journal of Marine Science 28, 76-78. (in Chinese)

Yuan, X. Y. and D. L. Xu (2006). Application Study of Denmark MIKE21 Model on Bridge Crossing Backwater Calculation. Journal of Yangtze River, 37, 31-32. (in Chinese)

Zhang, Y. L., A. M. Baptista and E. P. Myers (2004). A cross-scale model for

3D baroclinic circulation in estuary-plume-shelf systems: I Formulation and skill assessment. Continental Shelf Research 24, 2187-2214.

Zhang, W., B. Wang and H. F. Xia (2007). The Impact of the Air Blower Pile Group Layout in Offshore Wind Farm on Marine Hydrodynamic Conditions. Journal of China Harbour Construction 1, 1-4. (in Chinese)